



Transient Grounding Characteristic of Wind Turbines Affecting Back-flow Lightning Current into Distribution System

Kazuo Yamamoto, Yuki Kubo and Shinichi Sumi

Dept. of Electrical Engineering
Chubu University
Kasugai, Japan

Abstract—Lightning damages to facilities inside or in the vicinity of wind turbines become remarkably common. Most of the breakdowns and malfunctions of the electrical and control systems inside or in the vicinity of wind turbines are caused by ground potential rise due to lightning current flowing into the grounding system of the turbine and back-flow lightning current due to the ground potential rise. To clarify the transient characteristics of the wind turbine grounding systems and to understand the mechanism of the breakdowns and malfunctions, we have carried out a lot of field tests and simulations. In this paper, transient grounding characteristics of a wind turbines foundation are discussed

Keywords: wind turbine, grounding, transient, potential rise, foundation, lightning, Back-flow lightning current

I. INTRODUCTION

In recent years, accidents associated with the use of a large number of wind turbine generator systems have increased in number. Especially, lightning causes extensive and serious damage to these systems [1-6].

In order to exploit high wind conditions, wind turbine generator systems are often constructed on hilly terrain or along the seashore, where few tall structures exist in their vicinity; therefore, these structures are often struck by lightning. In order to promote wind power generation, it is important to understand the mechanism of the extensive and serious damage and to establish lightning protection methodologies for wind turbine generator systems [7].

Damage caused to wind turbine generator systems due to lightning affects the safety and reliability of these systems. Most of the breakdowns and malfunctions of the electrical and control systems inside or in the vicinity of wind turbines are caused by ground potential rise due to lightning and back-flow lightning current due to the ground potential rise [8, 9]. To solve the mechanism of generation of the potential rise in these multifarious ground systems, impulse tests at many kinds of wind turbine sites are necessary [10-26].

So far, the measurements of transient grounding characteristics carried out at wind turbines [10-26] have been described. Some of The measured grounding characteristics have already been verified [16-26] using the FDTD (finite-difference time-domain) method [21, 22]. From those measured and simulation results, it has been obvious that those grounding characteristics really depend on the size of the foundations, wave front duration of lightning current and grounding resistivity. In this paper, those relationships are discussed

II. FOUNDATION OF A WIND TURBINE

There are two types of wind turbine foundations. One of them is the square type that the top and bottom surfaces of the foundation are square, and the other type is octagonal. Fig. 1

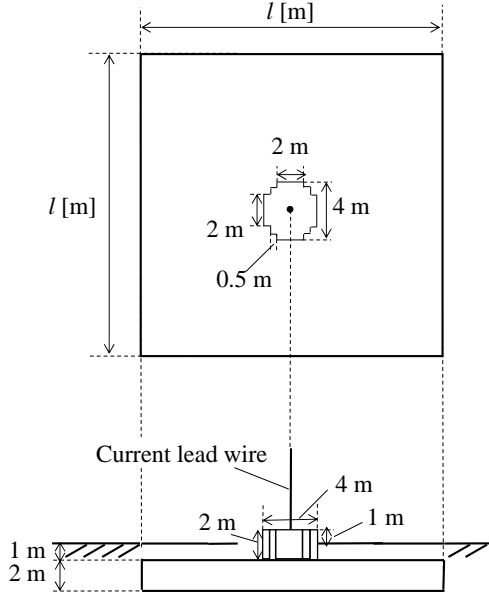


(a) Overall view

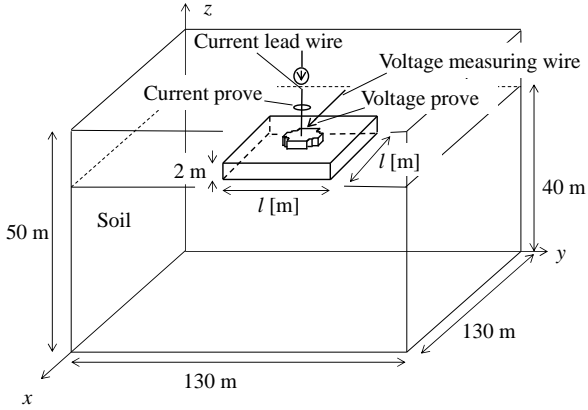


(b) Enlarged view

Fig. 1. Foundation before pouring concrete into the mold



(a) Foundation model in the case of $l \text{ m} \times l \text{ m}$



(b) Analytical space.

Fig. 2. Simulation model

shows an octagonal-type foundation before pouring concrete in to the mold. As shown in these pictures, the foundation consists of many reinforcing bars. Therefore, the foundation acts as a good grounding electrode. For the purposes of lightning protections, any other grounding electrodes usually are not required to fulfill the required grounding resistance of 10Ω [2].

III. ANALYTICAL MODEL

A. Analytical models and cases

The analytical model shown in Fig. 2 is utilized in this paper. When the current $I_i(t)$ is injected from the top of the foundation, the potential rise $V_p(t)$ are analyzed. The characteristics of $V_p(t_1)/I_i(t_2)$ (called ‘‘Impulse impedance’’, where t_1 : time when V_p is maximum and t_2 : time when I_i is maximum) and steady-state values of $V_p(t)/I_i(t)$ (called ‘‘Grounding resistance’’), and $V_p(t_1)/I_i(t_1)$ are studied. The sides of the foundation have been

changed to 10, 15 and 20m, the grounding resistivity and wave front duration are also varied from 0.1 to 10,000 Ωm and 0.5 to 82.5 μs . The waveforms of the injected currents are like a step waveform with several kinds of wave front durations shown in above.

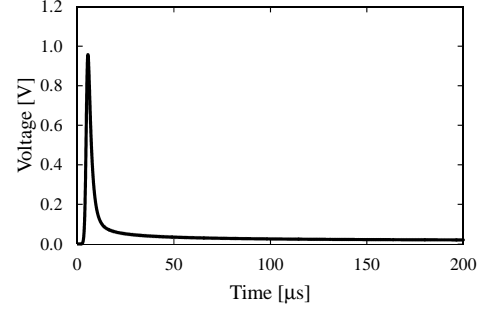


Fig. 3. Potential rise waveform (Size of foundation: $20 \text{ m} \times 20 \text{ m}$, grounding resistivity: $1 \Omega\text{m}$, wave front duration: $2.74 \mu\text{s}$).

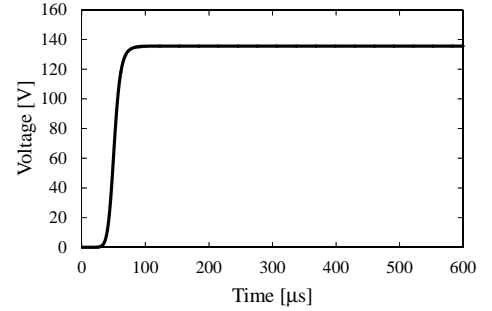


Fig. 4. Potential rise waveform (Size of foundation: $20 \text{ m} \times 20 \text{ m}$, grounding resistivity: $1000 \Omega\text{m}$, wave front duration: $27.5 \mu\text{s}$)

B. Analytical space

The FDTD analytical setup is shown in Fig. 2. The dimensions of the analytical space were $130 \text{ m} \times 130 \text{ m} \times 50 \text{ m}$, and it was divided into cube cells with a side length of 0.5 m. The absorbing boundary condition was 2nd order Liao.

The current source was connected between the foundation and current lead wire as shown in Fig. 2. The current lead wire and voltage measuring wire were connected to the absorbing boundaries. Thin-wire models to model the current lead and voltage measuring wires were used.

C. Features of the potential rise waveforms

When steep front current such as lightning is injected into a grounding system of a wind turbine, the potential rise appears depending on the grounding impedance of the grounding system. It may cause breakdowns and/or malfunctions at the instruments inside or in the vicinity of the wind turbine.

Fig. 3 shows the potential rise waveform when the current with the wave front duration of $2.74 \mu\text{s}$ is injected into the $20 \text{ m} \times 20 \text{ m}$ foundation buried in the ground where the ground resistivity is $1 \Omega\text{m}$. This potential rise has become inductive. On the other hands, Fig. 4 shows the potential rise waveform when the current with the wave front duration of $27.5 \mu\text{s}$ is injected into the same-size foundation buried in the ground where the ground resistivity is $1000 \Omega\text{m}$. This potential rise has shown capacitive. Depending on the ground resistivity, wave front duration and size of the foundation, those features appear.

D. Influences of the grounding resistivity

Fig. 5 shows the relations between impulse impedance and the grounding resistivity, when the current with several wave front durations of $0.5, 2.74, 13.4, 27.5$ and $82.5 \mu\text{s}$ and the peak of 1.0 A is injected into the $20 \text{ m} \times 20 \text{ m}$ foundation. In the cases of other scales of the foundations, same characteristics have been confirmed. Therefore, the explanations of the cases of $10 \text{ m} \times 10 \text{ m}$ and $14 \text{ m} \times 14 \text{ m}$ foundations are omitted. In Fig. 5, the data of $0.1, 1$ and $10 \Omega\text{m}$ in the wave front durations of $13.4 \mu\text{s}$ are the cases that the potential rises are inductive (white marks), and data of $100, 1,000$ and $10,000 \Omega\text{m}$ are the cases that the potential rises are capacitive (black marks). In each area, those features can be approximated linearly.

Fig. 6 shows the relations between the grounding resistance and the grounding resistivity. This characteristic includes only resistive feature of the grounding system. Therefore, the feature

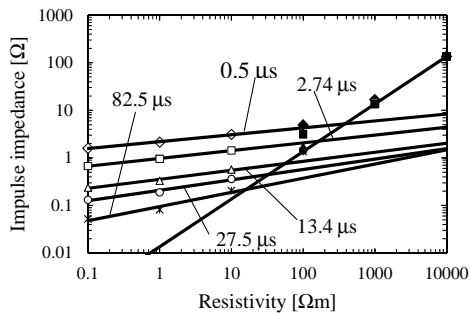


Fig. 5. Relation between impulse impedance and grounding resistivity (Size of foundation: $20 \text{ m} \times 20 \text{ m}$)

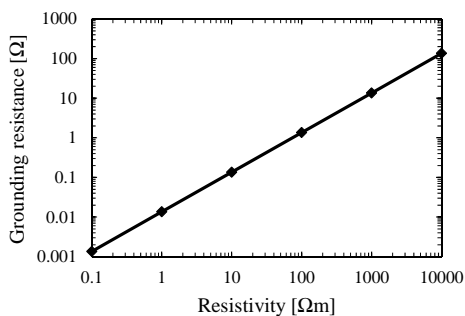


Fig. 6. Relation between grounding resistance and grounding resistivity (Size of foundation: $20 \text{ m} \times 20 \text{ m}$)

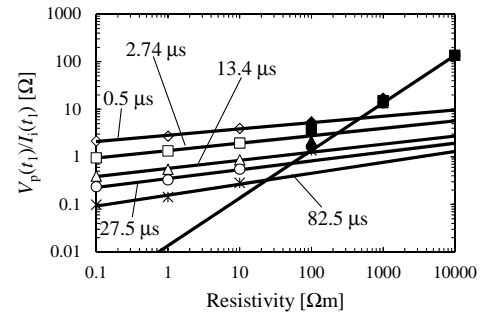


Fig. 7. Relation between $V_p(t_i)/I_i(t_i)$ and grounding resistivity (Size of foundation: $20 \text{ m} \times 20 \text{ m}$)

is in proportion to the value of the ground resistivity and does not depend on the values of the wave front duration.

Fig. 7 shows the relations between the values of $V_p(t_i)/I_i(t_i)$ and the grounding resistivity. In Fig. 7, the white marks are the cases that the maximum values of V_p appear at the wave front, and the black marks are the case that the maximum value of V_p appears at the wave tail.

E. Influences of the wave front duration

Fig. 8 shows the relations between the impulse impedance and the wave front duration of the injected current, when the current with the peak of 1.0 A is injected into the foundation buried in the ground where the grounding resistivity is $100 \Omega\text{m}$. In the cases of other grounding resistivity, same characteristics have been confirmed. Therefore, the results in case of $100 \Omega\text{m}$ is discussed. In Fig. 8, when the wave front duration is less than $20 \mu\text{s}$, the potential rises are inductive. Therefore, the peak values also appeared at the wave front. The peak values are in inverse proportion to the wave front duration.

Fig. 9 shows the relations between the grounding resistance and the wave front duration of the injected current, when the current with the peak of 1.0 A is injected into the foundation buried in the ground where the grounding resistivity is $100 \Omega\text{m}$. The steady-state values do not change depending on the wave front duration because the values only depend on the resistive component of the grounding impedance (namely, the grounding resistance).

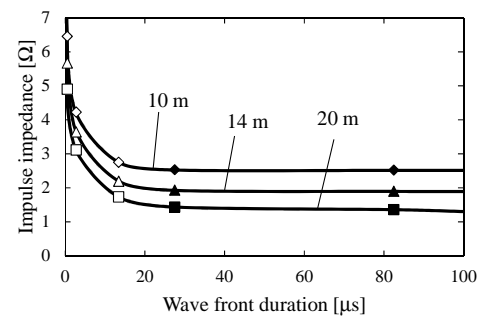


Fig. 8. Relation between impulse impedance and wave front duration (Size of foundation: $10 \text{ m} \times 10 \text{ m}$, $14 \text{ m} \times 14 \text{ m}$ and $20 \text{ m} \times 20 \text{ m}$, Grounding resistivity: $100 \Omega\text{m}$)

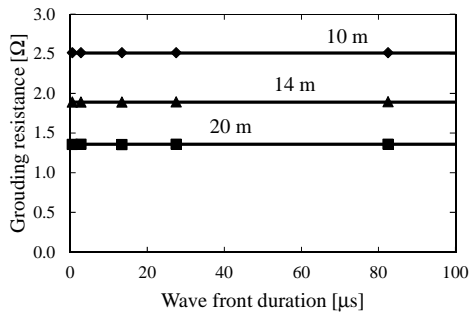


Fig. 9. Relation between grounding resistance and wave front duration (Size of foundation: 10 m × 10 m, 14 m × 14 m and 20 m × 20 m, Grounding resistivity: 100 Ωm)

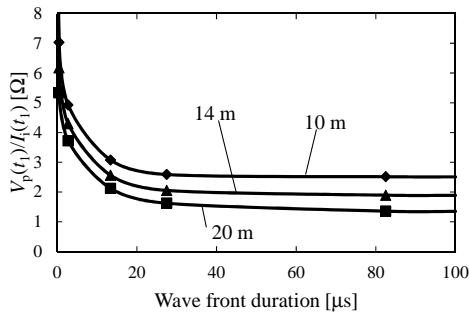


Fig. 10. Relation between values of $V_p(t_f)/I_i(t_f)$ and wave front duration (Size of foundation: 10 m × 10 m, 14 m × 14 m and 20 m × 20 m, Grounding resistivity: 100 Ωm)

The relations between the values of $V_p(t_f)/I_i(t_f)$ and the wave front duration of the injected current in Fig. 8 are also similar characteristic with the relation between impulse impedance and wave front duration as shown in Fig. 10.

IV. CONCLUSIONS

In this paper, the grounding characteristics of the wind turbine foundation have been shown by using the FDTD method, and the influences of the size of the foundation, the wave front duration of lightning current and the grounding resistivity on the grounding characteristics have been clarified.

The characteristics shown in this paper are useful for grounding designs of wind turbines. Our one of the next purposes is to derive simple equations from these characteristics.

REFERENCES

[1] I. Cotton, B. McNiff, T. Soerenson, W. Zischank, P. Christiansen, M. Hoppe-Kilpper, S. Ramakers, P. Pettersson and E. Muljadi: "Lightning Protection for Wind Turbines", in Proc. 25th International Conference on Lightning Protection, pp. 848–853, Rhodes, Greece (2000)

[2] IEC 61400-24, Wind Turbine Generator Systems-Part 24: Lightning protection (2010)

[3] NEDO, "Wind Turbine Failures and Troubles Investigating Committee Annual Report", (2006) (in Japanese).

[4] NEDO, "Wind Turbine Failures and Troubles Investigating Committee Annual Report", (2007) (in Japanese).

[5] J. Ribrant et al.: "Survey of Failures in Wind Power systems With Focus on Swedish Wind Power Plants During 1997-2005", IEEE Transactions on Energy Conversion, Vol. 22, No. 1, pp 167-173 (2007-3)

[6] F. Rachidi et al.: "A Review of Current Issues in Lightning Protection of New-Generation Wind-Turbine Blades", IEEE Transactions on Industrial Electronics, Vol. 55, No. 6, pp 2489-2496 (2008-6)

[7] J. Montanyà, O. van der Velde, and E. R. Williams: "Lightning discharges produced by wind turbines," J. Geophys. Res. Atmos., 119, pp. 1455–1462 (2014)

[8] K. Yamamoto, T. Noda, S. Yokoyama and A. Ametani: "An experimental study of lightning overvoltages in wind turbine generation systems using a reduced-size model", Electrical Engineering in Japan, Volume 158, Issue 4, pp. 22-30 (2007-3)

[9] K. Yamamoto, T. Noda, S. Yokoyama and A. Ametani: "Experimental and Analytical Studies of Lightning Overvoltages in Wind Turbine Generator Systems", Electric Power Systems Research Vol. 79, Issue 3, pp. 436-442, ISSN:0378-7796 (2009-3)

[10] K. Yamamoto, S. Yanagawa, S. Sekioka and S. Yokoyama, "Transient Grounding Characteristics of an Actual Wind Turbine Generator System at a Low Resistivity Site," IEEJ Transactions on Electrical and Electronic Engineering, Vol. 5, No. 1, pp 21-26 (2010-1)

[11] N. Ueda, A. Ametani, S. Yanagawa and K. Yamamoto, "Transient Grounding Characteristics of a Wind Turbine Generator System at a high resistivity site," Institute of Electrical Engineers of Japan, Research Meeting of High Voltage Engineering, HV-10-086, pp 23-28 (2010-12) (in Japanese)

[12] K. Yamamoto and S. Yanagawa, "Measurements of Transient Grounding Characteristics at a Wind Turbine under Construction", ISWL2011: 3rd International Symposium on Winter Lightning, No. 3-4, pp. 97-101 (2011-6)

[13] K. Yamamoto, S. Yanagawa and T. Ueda, "Field Tests of Grounding at an Actual Wind Turbine Generator System," International Conference on Lightning Protection (ICLP), No. 1307, Cagliari, Italy (2010-9)

[14] K. Yamamoto and S. Yanagawa, "Experimental Studies of Transient Grounding Characteristics of a Wind Turbine - Effectiveness of Counterpoises and a Ring Earth Electrode -,," Institute of Electrical Engineers of Japan, Research Meeting of High Voltage Engineering, HV-10-087, pp 29-34 (2010-12) (in Japanese)

[15] S. Yanagawa, D. Natsuno and K. Yamamoto, "A Measurement of Transient Grounding Characteristics of a Wind Turbine Generator System and its Considerations", Asia-Pacific International Conference on Lightning (APL), pp 401-404, Chengdu, China (2011-11)

[16] J. Niihara, A. Ametani and K. Yamamoto, "Transient Grounding Characteristics at a Wind Turbine with a Counterpoise", Asia-Pacific Symposium on Electromagnetic Compatibility (APEMC), Singapore (2012-5) Site 1

[17] K. Yamamoto, S. Sumi, S. Yanagawa and D. Natsuno "Transient Grounding Characteristic of a 600 kW Class Wind Turbine", 2012 CIGRE SC C4 Colloquium in Japan, No. III-4, pp.79-84 (2012-10) : Site 2

[18] S. Yanagawa, D. Natsuno and K. Yamamoto, "An Analytical Surveys of Transient Grounding Characteristics of a Wind Turbine Generator System and its Considerations", International Conference on Lightning Protection (ICLP), Vienna, Austria (2012-9) : Site 3

[19] Kazuo Yamamoto, Shinichi Sumi and Shunichi Yanagawa "Transient Characteristic of an Actual Wind Turbine Grounding System", 2013 Asia-Pacific Symposium on Electromagnetic Compatibility & Technical Exhibition on EMC, RF/Microwave Measurement & Instrumentation (2013-5) : Site 4

[20] Kazuo Yamamoto and Shinichi Sumi, "Validations of Lightning Protections for Accidents at a Wind Farm", XII SIPDA: International Symposium on Lightning Protection, pp. 412-417 (2013-10) : Site 5

[21] K. Yamamoto, S. Yanagawa, K. Yamabuki, S. Sekioka, S. Yokoyama, "Analytical Surveys of Transient and Frequency Dependent Grounding

- Characteristics of a Wind Turbine Generator System on the Basis of Field Tests”, IEEE Transactions on Power Delivery, Vol. 25, Issue 4, pp 3034-3043 (2010-10) Site 6
- [22] K. Yamamoto, J. Niihara and S. Yanagawa “Grounding Characteristics of a Wind Turbine Measured Immediately after Its Undergrounding”, 2012 Asia-pacific Symposium on Electromagnetic Compatibility & Technical Exhibition on EMC, RF/Microwave Measurement & Instrumentation (2012-5) : Site 7
- [23] K. Yamamoto, S. Yanagawa and T. Ueda, “Verifications of Transient Grounding Impedance Measurements of a Wind Turbine Generator System Using the FDTD method”, XI SIPDA: International Symposium on Lightning Protection, pp. 308-313 (2011-10) : Site 8
- [24] Kazuo Yamamoto and Shinichi Sumi, “Transient Grounding Characteristics of a Wind Turbine Foundation with Grounding Wires and Plates”, 2014 IEEE International Symposium on Electromagnetic Compatibility, pp. 570-575 (2014-8) : Site 9
- [25] Naoki Yoshikawa, Akihiro Ametani, Kazuo Yamamoto and Shunichi Yanagawa “Improvement of Wind Turbine Grounding System Using Various Grounding Wires”, 2013 Asia-pacific Symposium on Electromagnetic Compatibility & Technical Exhibition on EMC, RF/Microwave Measurement & Instrumentation (2013-5) : Site 10
- [26] Rafael Alipio, Silverio Visacro and Kazuo Yamamoto, “Lightning Response of Wind-Turbine Grounding System: Experimental and Simulated Results with Frequency-Dependent Soil Parameters”, APL2015: 9th Asia-Pacific International Conference on Lightning (2015-6): to be published : Site 11
- [27] K. S. Yee, J. S. Chen, and A. H. Chang: “Conformal finite-difference time-domain (FDTD) with overlapping grids”, IEEE Trans. Antennas Propag., vol. 40, pp. 1068-1075 (1992)
- [28] T. Noda and S. Yokoyama, “Thin wire representation in finite difference time domain surge simulation,” IEEE Trans. Power Delivery, vol. 17, pp. 840–847, July 2002.